

Analysis and Optimization Design of Snubber Circuit for Isolated DC-DC Converters in DC Power Grid

Koji Orikiawa

Nagaoka University of Technology
Nagaoka, Japan
orikawa@stn.nagaokaut.ac.jp

Jun-ichi Itoh

Nagaoka University of Technology
Nagaoka, Japan
itoh@vos.nagaokaut.ac.jp

Abstract—This paper clarifies the principle of the surge voltage in the diode rectifier that is connected to the transformer in the isolated DC-DC converter. In addition, the design method of the RC snubber circuit is discussed by using the equivalent circuit that is consisting of the transformer, the snubber circuit and the diode. Finally, the experimental results are provided to validate the design method.

Keywords—component; Smart grid; DC power grid; Isolated DC-DC converters; Rectifier diode; Surge voltage; Snubber circuit

I. INTRODUCTION

Recently, the DC interface converters for the smart grid have attracted large attentions in community. The size and efficiency of high power DC-DC converters become particularly important especially for the photovoltaic generation and battery storage system. On the other hand, the developing of wide-gap semiconductor such as silicon carbide (SiC) and gallium nitride (GaN), which is the high switching frequency semiconductor devices, have been actively progressing. Therefore, packaging technologies for power converters that feature small size and high-density are highly researching [1]-[2]. However, the occurrence of surge voltage during high frequency switching in the semiconductor switching devices is one of the known problems. The surge voltage induces problems such as overvoltage and high frequency noises in the semiconductor switching devices. As the result, breakdown and malfunction in the semiconductor switching devices could be happen in the power converters such as the high power DC-DC converters for the smart grid. Therefore, the suppression on the surge voltage is an important aspect to study in order to offer high reliability in a power supply system.

Isolated DC-DC converters using transformers have been studying actively [3]. Because the transformer can insulate transform voltage into an AC voltage easily. The surge voltage generally occurs in the output rectifier diodes that is connected to the output of transformer. It is known that the surge voltage in the output rectifier diode is caused by the leakage inductance of the transformer, and a parasitic capacitance of the diode. However, there have been few quantitative discussions only on the design of the snubber circuit based on the principle of the surge voltage in the diode [4]-[6]. As the result, the design of

the snubber circuit is basically depending on the experiences of designers.

This paper clarifies the principle of the surge voltage in the output diode rectifier that is connected to the isolated DC-DC converters with consideration of the design method in the RC snubber circuit, which is connected to the secondary side of the transformer. A theoretical equation of the surge voltage is derived from the equivalent circuit. Snubber circuit parameters are designed based on a parasitic capacitance and the power consumption of the snubber circuit. At the end, the validity of the design method is confirmed from the experimental results.

II. PRINCIPLE OF SURGE VOLTAGE ON DIODE

Fig. 1 shows a circuit diagram of the isolated DC-DC converter which is investigated in this paper. This circuit consists of a single phase inverter, a high frequency transformer, a diode rectifier and a R load. In this experiment, the inverter is operated with the square waveform drive.

A. Equivalent Circuit

Fig. 2(a) shows the equivalent circuit when the surge voltage occurs in the diode D_1 after the overlapping period during commutation from D_3 to D_1 . The current path is illustrated with a dot line. R is a wiring resistance of the transformer. L is a leakage inductance of the transformer. Fig. 2(b) and (c) show simulation waveforms of Fig. 2(a). The value of wiring resistance and leakage inductance of the primary side of the transformer is converted to the secondary side of the transformer. In addition, the characteristic of the actual diode is demonstrated with the ideal diode, on resistance R_{on} , off resistance R_{Doff} , the forward voltage V_F and the parasitic capacitance C . The output current cannot change rapidly because of a smooth inductance L_{out} . As the result, the rush current flows through the parasitic capacitance. In addition, the vibrational current flows through the leakage inductance which

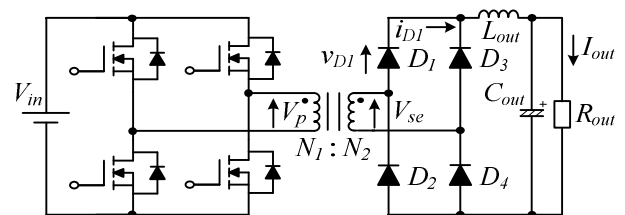


Figure 1. Full bridge isolated DC-DC converter.

results the reverse electromotive voltage occurs in the leakage inductance. That is, the reverse electromotive voltage of the leakage inductance becomes the surge voltage. Therefore, the surge voltage does not occur when the ideal transformer which has no leakage inductance is used.

From the principle which is mentioned above, in order to reduce the surge voltage, it is needed to suppress the rush current in the parasitic capacitance. An energy buffer is an effective method to suppress the rush current in the parasitic capacitance.

B. Theoretical Analysis of Surge Voltage

Theoretical equation of the surge voltage is derived from the equivalent circuit as shown in Fig. 2(a). Table 1 shows the conditions of the simulation circuit. The theoretical equation of the surge voltage is given by (1).

$$v_{D1max} = I_{st} R_{Doff} \left\{ 1 + e^{-\tau/(2f_{vib})} \right\} - V_F. \quad (1)$$

where I_{st} is the steady current of the diode when diode is turned off, τ is the damping time constant and f_{vib} is the vibrational frequency of the surge voltage. I_{st} , τ and f_{vib} are given by (2), (3), (4).

$$I_{st} = \left\{ V_{se} - I_{out} (R + R_{Don}) \right\} / (2R + R_{Don} + R_{Doff}). \quad (2)$$

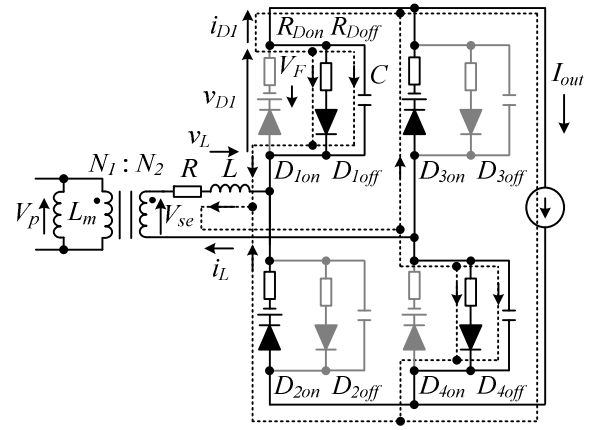
$$\tau = \left\{ CRR_{Doff} + (CR_{Don}R_{Doff}) / 2 + L \right\} / (2LCR_{Doff}). \quad (3)$$

$$f_{vib} = \sqrt{(2R + R_{Don} + R_{Doff}) / (2LCR_{Doff}) - \tau^2} / (2\pi). \quad (4)$$

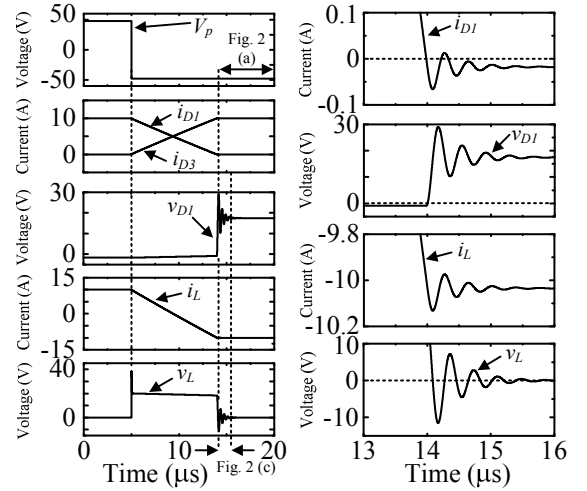
where V_{se} is the secondary side voltage of the transformer and I_{out} is the output current. From (1), it is confirmed that the surge voltage depends on (2), (3) and (4) which are changed by the parameters; the wiring resistance, the leakage inductance and the parasitic capacitance.

In order to confirm the validity of the equations which are shown in (1) and (4) respectively, the calculation results of (1) and (4) are shown in Fig. (3) and Fig. (4) in the case that the leakage inductance L and the parasitic capacitance C are changed respectively.

Fig. 3 shows the theoretical waveforms of the diode voltage and the surge voltage in the case that the leakage inductance L is changed. From Fig. 3, it is confirmed that the vibrational frequency decreases and the surge voltage is reduced according to increment of the leakage inductance L . The reason that the surge voltage reduced are follows; by increasing the leakage inductance, the impedance of the series circuit which consists of the leakage inductance and the parasitic capacitance are increased. As a result, the rush current of the parasitic capacitance is reduced which also reduce the surge voltage. This means the damping time constant and vibrational frequency that is shown in (3) and (4) are changed, then the



(a) When surge voltage occur in D_1 .



(b) Voltage and current waveforms. (c) Enlarged waveforms. Figure 2. Equivalent circuit of secondary part in Fig. 1.

TABLE I. CONDITIONS OF SIMULATION CIRCUIT

| | |
|---------------------------------|----------------------|
| Input voltage V_{in} | 48 (V) |
| Output current source I_{out} | 10 (A) |
| Output inductance L_{out} | 0.5 (mH) |
| Output capacitance | 2200 (μ F) |
| Switching frequency f_{sw} | 20 (kHz) |
| Winding resistance R | 53 (m Ω) |
| Leakage inductance L | 8.6 (μ H) |
| Turn ratio n | $n=N_1/N_2=15/6=2.5$ |
| Parasitic capacitance C | 200 (pF) |
| On resistance R_{Don} | 0.086 (Ω) |
| Off resistance R_{Doff} | 1 (k Ω) |
| Forward voltage V_F | 0.86 (V) |

power of an exponential in (1) will increase by increasing of the leakage inductance. As a result, the di_L/dt of the leakage inductance current decreases, and the reverse electromotive voltage occurs in the leakage inductance is reduced. Therefore, the surge voltage is reduced.

Fig. 4 shows theoretical waveforms of the diode voltage and the surge voltage in the case that the parasitic capacitance C is changed. From Fig. 4, it is confirmed that the vibrational frequency decreases and the surge voltage is reduced according to increment of the parasitic capacitance C . This reason is that the impedance of the series circuit which consists of the

leakage inductance and the parasitic capacitance are increase. As a result, the rush current of the parasitic capacitance becomes larger. That is the di_L/dt of the leakage inductance current increases which result the reverse electromotive voltage occurs in the leakage inductance increases. Therefore, the surge voltage increases.

III. SURGE VOLTAGE IN THE EXPERIMENT

In order to confirm the validity of the theoretical analysis, the surge voltage in the diode of the prototype circuit is measured and compared with the theoretical analysis.

A. Changes of Leakage Inductance

In this experiment, the air-core reactor which has same resistance but different inductance, are connected to the secondary side of the transformer in series. By using this method, the damping effect by the winding resistance R can be neglected. The effect of the leakage inductance on the surge voltage only can be measured.

Fig. 5(a) shows the experimental waveforms consists of the following, the primary side voltage of the transformer, the diode current and the diode voltage without the snubber circuit. After the primary side voltage of the transformer changes from a positive value to a negative value, the overlapping period occurs in the commutation. Also, it is confirmed that the surge voltage occurs in the diode. Fig. 5(b) shows the waveforms of the diode current and diode voltage in the case that the leakage inductance L is changed. From Fig. 5(b), it is seen that the vibrational frequency and the surge voltage decreases according to the increment of the leakage inductance L .

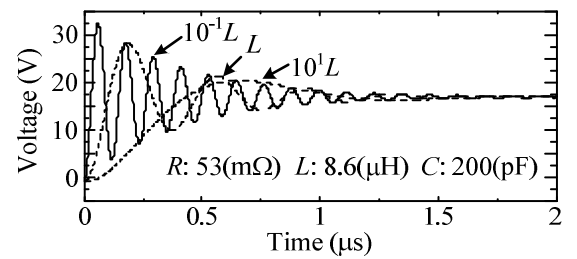
Fig. 6 shows the comparison between the theoretical and experimental values, which are subjected to the ratio between the surge voltage and steady voltage. In the case of the experiment, the characteristic of the vibrational frequency and the surge voltage are similar to the theoretical value. Therefore, the experimental results can confirm that the investigation in the equivalent circuit is valid.

B. Changes of Parasitic Capacitance

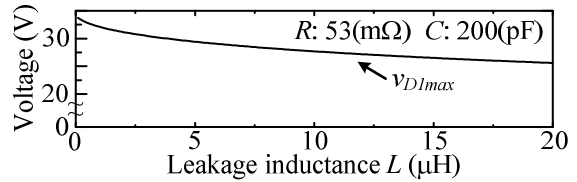
In this experiment, the parasitic capacitance is changed by connecting the capacitance to the diode in parallel.

Fig. 5(c) shows the waveforms, the diode current and diode voltage in the case that the parasitic capacitance C is changed. From Fig. 5(c), it can be seen that the vibrational frequency and the surge voltage decreases according to increment of the parasitic capacitance C .

Fig. 7 shows the comparison between the theoretical and experimental values which are subjected to the ratio between the surge voltage and steady voltage. In the case of the experiment, the characteristic of the vibrational frequency is similar to the theoretical value. On the other hand, the characteristic of the surge voltage which is based on the theoretical is different from the experimental results as seen in Fig. 7 (b). This reason is that the capacitance which is connected to the diode in parallel and its wiring resistance works as the snubber circuit. As a result, in contrast to the

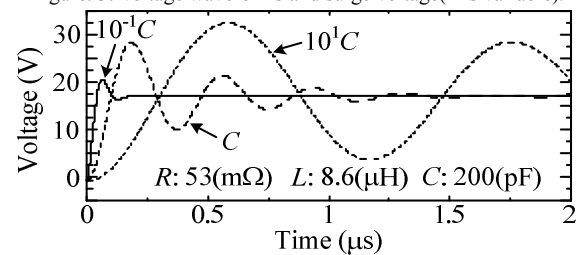


(a) Voltage waveform of the diode.

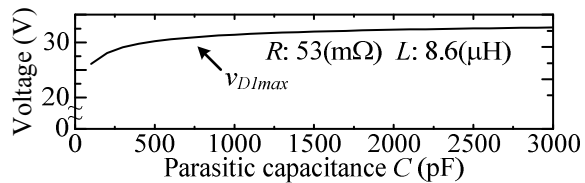


(b) Surge voltage of the diode.

Figure 3. Voltage waveforms and surge voltage (L is variable).



(a) Voltage waveform of the diode.



(b) Surge voltage of the diode.

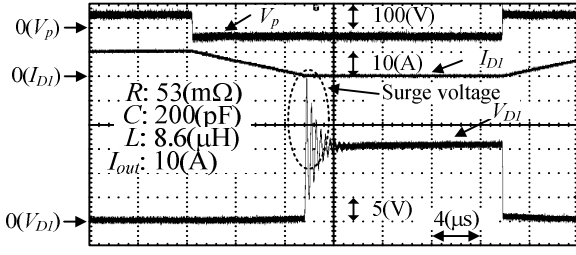
Figure 4. Voltage waveforms and surge voltage (C is variable).

theoretical analysis, the surge voltage can be suppressed in the experiment.

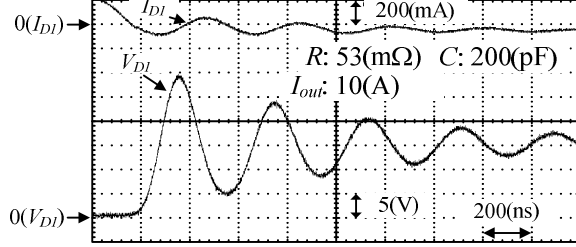
In according to the considerations which are mentioned above, the required conditions for suppressing the surge voltage by reducing the rush current of the parasitic capacitance are shown below.

- 1) Winding resistance of the transformer : Large
- 2) Leakage inductance of the transformer : Large
- 3) Parasitic capacitance of the diode : Small

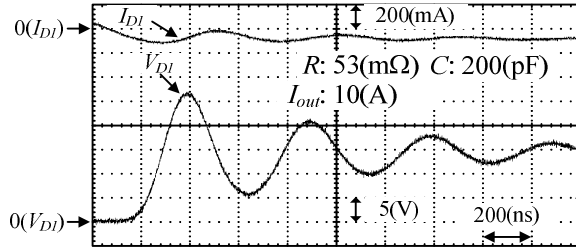
However, in general the winding resistance of the transformer is low in order to reduce the copper loss. The leakage inductance is also low except the application which the leakage inductance is used in a positive way. Therefore, a trade-off relationship that is subjected to reduce the surge voltage is established between i) to achieve a low wiring resistance and ii) to achieve a low leakage inductance. On the other hand, the parasitic capacitance depends on the rating of the voltage and current. Therefore, it is difficult to always select the diode which has a small parasitic capacitance.



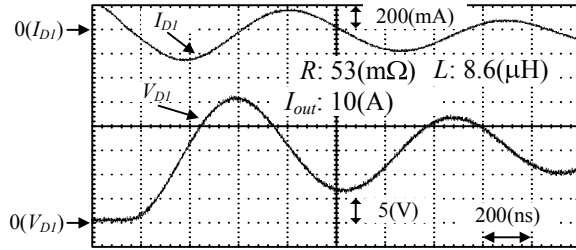
(a) Voltage and current waveform ($L: 8.6\mu\text{H}$, $C: 200\text{pF}$).



(b) Enlarged waveform of Fig. 5 (a) ($L: 8.6\mu\text{H}$, $C: 200\text{pF}$).



(c) Enlarged voltage and current waveform ($L: 15.9\mu\text{H}$, $C: 200\text{pF}$).



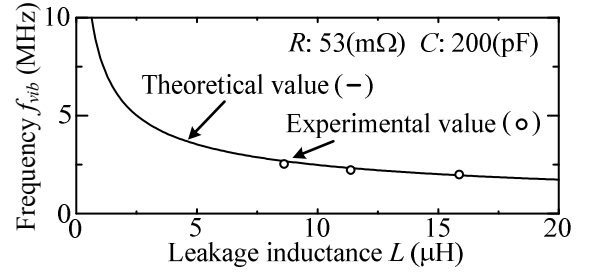
(d) Enlarged voltage and current waveform ($L: 8.6\mu\text{H}$, $C: 200\text{pF}$).

Figure 5. Experimental waveforms.

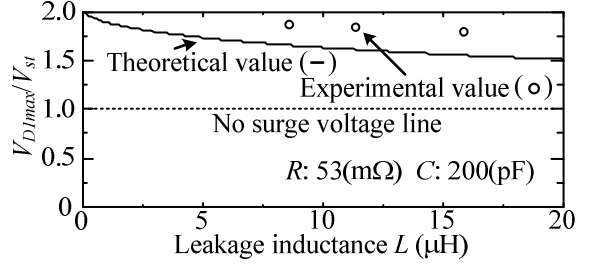
IV. DESIGN METHOD OF SNUBBER CIRCUIT

As mentioned above, there are limitations to suppress the surge voltage by reducing the rush current of the parasitic capacitor from the design of transformer and selection of diode. Therefore, the snubber circuit is connected to the diode in parallel. It consists of the snubber resistance and the snubber capacitance which has a larger value than that of the parasitic capacitance. By using the snubber circuit, the surge voltage can be reduced by reducing the rush current of the parasitic capacitance. This paper describes the design of a RC snubber circuit which is connected to the secondary side of the transformer.

Fig. 8 shows the equivalent circuit of Fig. 2(a) in case that the common snubber circuit is connected to the secondary side of the transformer. The snubber circuit is designed based on Fig. 8. In particular, Fig. 8 is divided into two parts: the dotted line region which consists of the transformer and the snubber circuit and the equivalent circuit of the diode. Firstly, the peak

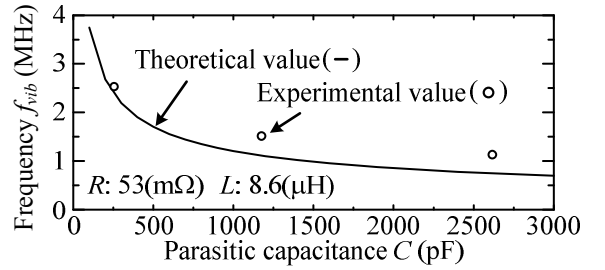


(a) Vibrational frequency as a function of the leakage inductance.

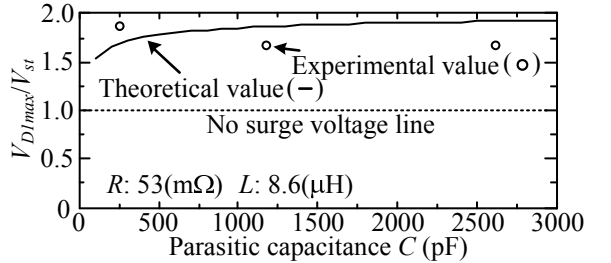


(b) Ratio between surge voltage and steady voltage.

Figure 6. Theoretical value and experimental value of the surge voltage and the vibrational frequency (L is variable).



(a) Vibrational frequency as a function of the parasitic capacitance.



(b) Ratio between surge voltage and steady voltage.

Figure 7. Theoretical value and experimental value of the surge voltage and the vibrational frequency (C is variable).

value of the step response in the dotted line circuit is calculated. After that, subtracting the voltage drop of the diode from it, these calculation results become the designed value of the surge voltage $V_{DI,snmax}$. The coefficient that the designed value of the surge voltage divided by the steady voltage V_{st} is given by (5).

$$V_{DI,snmax} / V_{st} = V_{se} [1 + e^{-k}] / V_{st} - (I_{out} R_{Don} + V_F) / V_{st}. \quad (5)$$

where V_{st} is the steady voltage, k is a constant value. k is given by (6).

$$k = \frac{\zeta}{\sqrt{1-\zeta^2}} \left[\tan^{-1} \left\{ \frac{\sqrt{1-\zeta^2}(1-4\zeta^2)}{\zeta(3-4\zeta^2)} \right\} - \tan^{-1} \left(\frac{\sqrt{1-\zeta^2}}{\zeta} \right) + \pi \right] \quad (6)$$

From (5), the surge voltage will be determined in case that the output current and the parameters of the diode are known. In addition, the relationship among the snubber resistance R_{sn} , the snubber capacitance C_{sn} and the damping coefficient ζ are given by (7).

$$R_{sn} = 2\zeta\sqrt{L/C_{sn}}. \quad (7)$$

From (7), the snubber resistance R_{sn} can be designed after the snubber capacitance C_{sn} is determined. However, the number of the combination of two parameters is infinity. In this section, C_{sn} is designed based on the relationship among the snubber capacitance, the parasitic capacitance and the snubber loss. In the end, R_{sn} is designed using by (7).

In the case of the smaller snubber capacitance, the impedance of the snubber circuit increases, which results the snubber circuit does not work. Therefore, the snubber circuit cannot suppress the surge voltage. On the other hand, in case of the larger snubber capacitance, the impedance of the snubber circuit decreases. As a result, the snubber circuit can suppress the surge voltage. However, the snubber current and the power consumption of the snubber circuit increases. Therefore, the optimum value of the snubber capacitance needs to be identified according to the parasitic capacitance. The power consumption of the snubber circuit P_{sn} is given by (10) in the case that the dotted line region only is considered in Fig. 8.

$$P_{sn} = \frac{R_{sn}}{R_0^2} \sum \frac{\omega_n^2 / \omega_0^2}{(1 - \omega_n^2 / \omega_0^2)^2 + (\omega_n^2 / \omega_0^2)(R_{sn}^2 / R_0^2)} |V_{se}(\omega_n)|^2 \quad (8)$$

where ω_n is a n-order natural angular frequency of the secondary side voltage in the transformer. ω_n and R_0 are given by (9), (10).

$$\omega_0 = 1/\sqrt{LC_{sn}} \quad (9) \quad R_0 = \sqrt{L/C_{sn}} \quad (10)$$

Fig. 9 shows a flowchart of the snubber circuit design. Required parameters for the design of the snubber circuit are designed surge voltage $V_{DIsnmax}$, the output current I_{out} , on resistance R_{Don} , the forward voltage V_F , the parasitic capacitance C , the leakage inductance L and an allowance snubber loss P_{asn} . First, the damping coefficient ζ is decided by parameters which are mentioned above. Then, the snubber resistance R_{sn} is calculated by (7). In the end, if a calculated snubber loss P_{sn} is less than the allowance snubber loss, then the design of the snubber circuit is completed.

V. EXPERIMENTAL RESULTS WITH SNUBER CIRCUIT

Fig. 10 shows waveforms, the diode voltage and the current of the snubber circuit in the case that the ratio between the

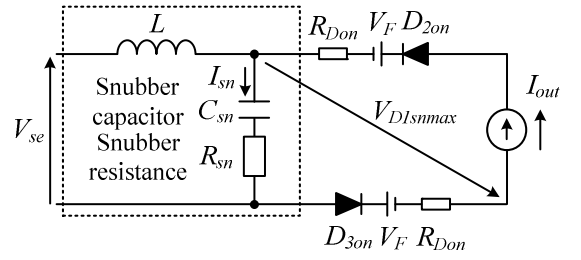


Figure 8. Equivalent circuit of the transformer with the RC snubber circuit.

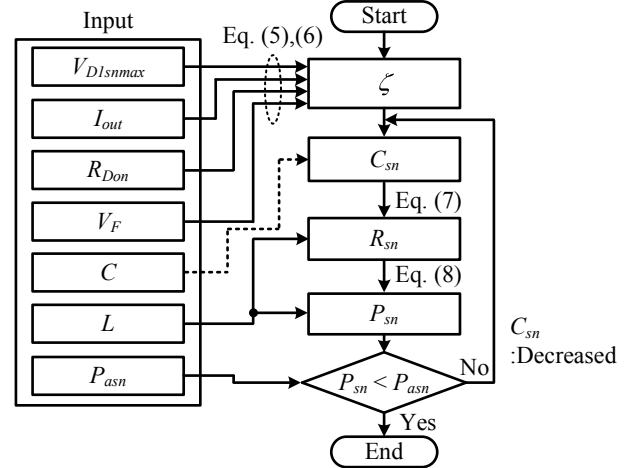
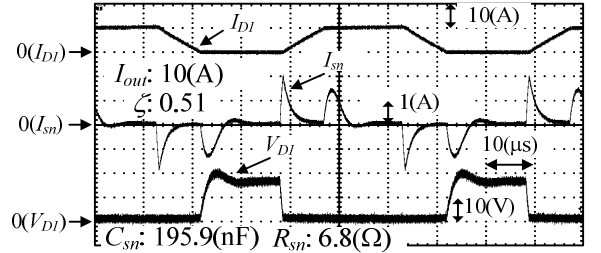
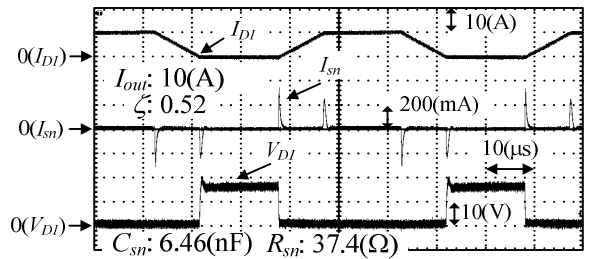


Figure 9. Flowchart for design of snubber circuit.



(a) $C/C_{sn}=10^{-3}$.

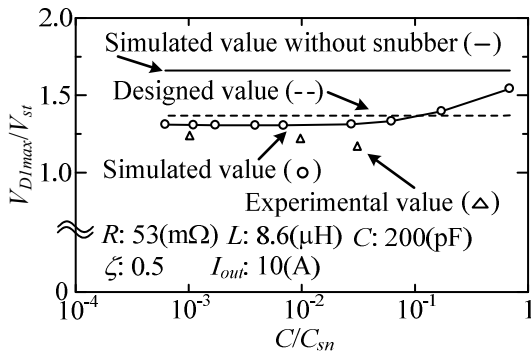


(b) $C/C_{sn}=3 \times 10^{-2}$.

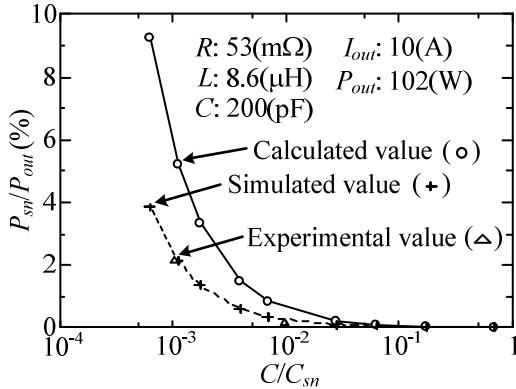
Figure 10. Waveforms of the diode and the current of the snubber.

parasitic capacitance and the snubber capacitance is changed under a constant damping coefficient. It can be seen that the surge voltage is almost same and the current of the snubber circuit increase according to the increment of the parasitic capacitance. Therefore, it is confirmed that the experimental results is well agreed with the theoretical analysis which are mentioned in the chapter IV.

Fig. 11(a) shows the designed value, the simulation results, and the experimental results in terms of the ratio between the surge voltage and steady voltage of the diode. Fig. 11(b) shows



(a) Ratio between surge voltage and steady voltage.



(b) Snubber loss.

Figure. 11. Ratio between surge voltage and steady voltage and snubber loss as a function of ratio between parasitic capacitance and snubber capacitance.

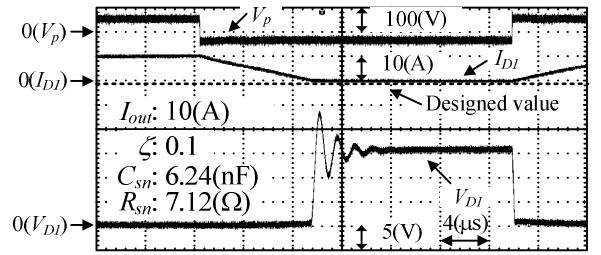
the calculation result which is obtained by (8), the simulation result is obtained by adding the RC snubber circuit to Fig. 2(a), and the experimental result is obtained from Fig. 10 in terms of the power consumption of the snubber circuit. From Fig. 11(a), it is confirmed that the snubber capacitance should be designed from 10 to 30 times larger than the parasitic capacitance. In addition, it is seen that the calculation result is larger than the simulation result. In other words, the worst case of the power consumption of the snubber circuit can be calculated by using (8)

Fig. 12 shows the experimental waveform with snubber circuit in the case that $C/C_{sn}=0.03$. From Fig. 12, it is confirmed that surge voltage is suppressed below than the designed value.

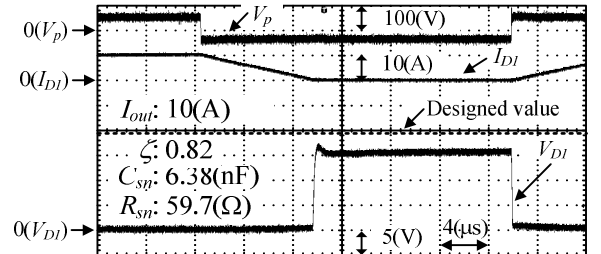
Fig. 13 shows the comparison between the designed and experimental values that are subjected to the ratio between the surge voltage and steady voltage. From Fig. 13, it is confirmed the tendency of the designed and experimental values is closed.

VI. CONCLUSION

This paper clarifies the principle of the surge voltage on the diode in the isolated DC-DC converter and also the design method of the snubber circuit that is connected to the secondary side of the transformer. It is confirmed that the surge voltage depends on the wiring resistance, the leakage inductance and the parasitic capacitance, based on the experimental results obtained from the equivalent circuit. In addition, it is confirmed that the surge voltage is suppressed



(a) With RC snubber ($\zeta:0.1$).



(b) With RC snubber ($\zeta:0.82$).

Figure. 12. Voltage waveforms of the diode without snubber and with snubber using designed parameter.

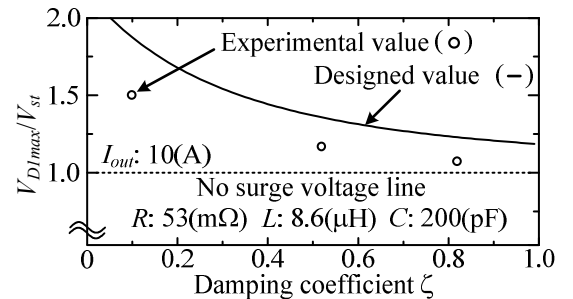


Figure. 13. Ratio between the surge voltage and the steady voltage.

below the designed value with the snubber circuit which has a low snubber loss. In the end, the validity of the analysis results, which is based on the equivalent circuit, has been confirmed by experimental results.

REFERENCES

- [1] J. Kondoh, T. Yatsuo, I. Ishii, K. Arai : "Estimation of Converters with SiC Devices for Distribution Networks", IEEJ Transaction on Industry Applications, Vol.126, No.4, pp.480-488 (2006)
- [2] Biela, J.; Aggeler, D.; Inoue, S.; Akagi, H.; Kolar, J.W. : "Bi-Directional Isolated DC-DC Converter for Next-Generation Power Distribution-Comparison of Converters Using Si and SiC Devices", IEEJ Transaction on Industry Applications, Vol.128, No.7, pp.901-909 (2008)
- [3] Simanjorang, R.; Yamaguchi, H.; Ohashi, H.; Takeda, T.; Yamazaki, M.; Murai, H. : "Low Cost Transformer Isolated Boost Half-bridge Micro-inverter for Single-phase Grid-connected Photovoltaic System", Applied Power Electronics Conference and Exposition (APEC) 2010, pp.648-653 (2010)
- [4] M. Hirokawa, T. Ninomiya: "Non-Dissipative Snubber for Rectifying Diodes in a High-Power DC-DC Converter", T.IEEJapan, Vol. 125-D, No. 4, pp.366-371(2005) (in Japanese)
- [5] D. Yoshitomi, J. Itoh, K. Hirachi: "Relationship between Leakage Inductance and Surge Voltage on Isolated DC-DC Converter", Japan Institute of Power Electronics, JIPE-37-3 (2011) (in Japanese)
- [6] Cacciato, M.; Consoli, A. : "New Regenerative Active Snubber Circuit for ZVS Phase Shift Full Bridge Converter", Applied Power Electronics Conference and Exposition (APEC) 2011, pp.1507-1511 (2011)